# Efficient beaming of self-collimated light from photonic crystals

**Jong-Moon Park, Sun-Goo Lee, Hae Yong Park, and Jae-Eun Kim**

*Department of Physics, KAIST, Daejeon 305-701, Korea*

*jekim@kaist.ac.kr*

**Abstract:** We propose a novel structure for achieving highly efficient beaming of self-collimated light from two-dimensional photonic crystals. The finite-difference time-domain simulations show that both enhanced transmission and highly directional emission of self-collimated beams from photonic crystals are achieved by using the bending and splitting of self-collimated beams in photonic crystals, and also by introducing an antireflection coating-like photonic crystal collimator to the exit surface of the structure. This structure is potentially important for highly efficient coupling of self-collimated beams from photonic crystals into conventional optical fibers and photonic crystal waveguides.



**OCIS codes:** (230.5298) Photonic crystals;(130.3120) Integrated optics devices; (250.5300) Photonic integrated circuits.

## References and links

1. J. D. Joannopoulos, R. D. Meade, and J. N. Winn, *Photonic Crystals: Molding the Flow of Light* ( Princeton University Press, Princeton, NJ, 1995).
2. A. Yariv, Y. Xu, R. K. Lee, and A. Scherer, "Coupled-resonator optical waveguide: a proposal and analysis," Opt. Lett. **24**, 711 (1999).
3. M. Bayindir, B.Temelkuran, and E. Ozbay, "Tight-Binding Description of the Coupled Defect Modes in Three-Dimensional Photonic Crystals," Phys. Rev. Lett. **84**, 2140 (2000).
4. Y. Fink, J. N. Winn, S. Fan, C. Chen, J. Michel, J. D. Joanopoulos, and E. L. Thomas, "A Dielectric Omnidirectional Reflector," Science **282**, 1679 (1998).
5. H. Kosaka, T. Kawashima, A. Tomita, M. Notomi, T. Tamamura, T. Sato, and S. Kawakami, "Self-collimating phenomena in photonic crystals," Appl. Phys. Lett. **74**, 1212 (1999).
6. J. Witzens, M. Loncar, and A. Scherer, "Self-collimation in Planar Photonic Crystals," IEEE J. Sel. Top. Quantum Electron. **8**, 1246 (2002).
7. X. Yu and S. Fan, "Bends and splitters for self-collimated beams in photonic crystals," Appl. Phys. Lett. **83**, 3251 (2003).
8. S.-G. Lee, S. S. Oh, J.-E. Kim, H. Y. Park, and C.-S. Kee, "Line-defect-induced bending and splitting of self-collimated beams in two-dimensional photonic crystals," Appl. Phys. Lett. **87**, 181106-1 (2005).
9. B. Miao, C. Chen, S. Shi, and D. W. Prather, "A high-efficiency in-plane splitting coupler for planar photonic crystal self-collimation devices," IEEE Photon. Technol. Lett. **17**, 61 (2005).
10. E. Moreno, F. J. García-Vidal, and L. Martín-Moreno, "Enhanced transmission and beaming of light via photonic crystal surface modes," Phys. Rev. B **69**, 121402-1 (2004).
11. P. Kramper, M. Agio, C. M. Soukoulis, A. Birner, F. Müller, R. B. Wehrspohn, U. Gösele, and V. Sandoghdar, "Highly dirctional emission from photonic crystal waveguides of subwavelength width," Phys. Rev. Lett. **92**, 113903 (2004).
12. S. K. Morrison and Y. S. Kivshar, "Engineering of directional emission from photonic-crystal waveguides," Appl. Phys. Lett. **86**, 081110 (2005).
13. C.-C. Chen, T. Pertsch, R. Iliew, F. Lederer, and A. Tünnermann, "Directional emission from photonic crystal waveguides," Opt. Express **14**, 2423 (2006).
14. Z.-H. Zhu, W.-M. Ye, J.-R. Ji, X.-D. Yuan, and C. Zen, "Enhanced transmission and directional emission via coupled-resonator optical waveguides," Appl. Phys. B **86**, 327 (2007).

#102911 - $15.00 USD Received 20 Oct 2008; revised 19 Nov 2008; accepted 21 Nov 2008; published 24 Nov 2008

15. D. Tang, L. Chen, and W. Ding, "Efficient beaming from photonic crystal waveguides via self-collimation effect," Appl. Phys. Lett., **89**, 131120 (2006).
16. Z. Li, K. Aydin, and E. Ozbay, "Highly directional emission from photonic crystals with a wide bandwidth," Appl. Phys. Lett. **91**, 121105 (2007).
17. A. Mekis, J. C. Chen, I. Kurland, S. Fan, P. R. Villeneuve, and J. D. Joannopoulos, "High Transmission through Sharp Bends in Photonic Crystal Waveguides," Phys. Rev. Lett. **77**, 3787 (1996).
18. M. Bayindir, E. Ozbay, B.Temelkuran, M. M. Sigalas, C. M. Soukoulis, R. Biswas, and K. M. Ho, "Guiding, bending, and splitting of electromagnetic waves in highly confined photonic crystal waveguides," Phys. Rev. B **63**, 081107 (2001).
19. Y. Zhang, Y. Zhang, and B. Li, "Highly-efficient directional emission from photonic crystal waveguides for coupling of freely propagated terahertz waves into Si slab waveguides," Opt. Express **15**, 9281 (2007).
20. Q. Wang, Y. Cui, C. Yan, L. Zhang, and J. Zhang, "Highly efficient directional emission using a coupled multi-channel structure to a photonic crystal waveguide with surface modification," J. Phys. D: Appl. Phys. **41**, 105110 (2008).
21. W. Y. Liang, J. W. Dong, and H. Z. Wang, "Directional emitter and beam splitter based on self-collimation effect," Opt. Express **15**, 1234 (2007).
22. S. G. Johnson and J. D. Joannopoulos, "Block-iterative frequency-domain methods for Maxwell's equations in a planewave basis," Opt. Express **8**, 173 (2001).
23. S.-G. Lee, J.-S. Choi, J.-E. Kim, H. Y. Park, and C.-S. Kee, "Reflection minimization at two-dimensional photonic crystal interfaces," Opt. Express **16**, 4270 (2008).
24. K. S. Yee, "Numerical solution of initial boundary problems involving Maxwell's equations in isotropic media," IEEE Trans. Antennas Propag. **AP-14**, 302 (1966).
25. A. Matthews and Y. Kivshar, "Tunable Goos-Hänchen shift for self-collimated beams in two-dimensional photonic crystals," Phys. Lett. A **372**, 3098 (2008).
26. D. Felbacq and R. Smaâli, "Bloch Modes Dressed by Evanescent Waves and the Generalized Goos-Hänchen Effect in Photonic Crystals," Phys. Rev. Lett. **92**, 193902-1 (2004).
27. Y. Zhang, Y. Zhang, and B. Li, "Optical switches and logic gates based on self-collimated beams in two-dimensional photonic crystals," Opt. Express **15**, 9287 (2007).
28. D. Zhao, J. Zhang, P. Yao, X. Ziang, and X. Chen, "Photonic crystal Mach-Zehnder interferometer based on self-collimation," Appl. Phys. Lett. **90**, 231114-1 (2007).
29. Z. Y. Ou and L. Mandel, "Derivation of reciprocity relations for a beam splitter from energy balance," Am. J. Phys. **57**, 66 (1989).
30. J. P. Berenger, "A perfectly matched layer for the absorption of electromagnetic waves," J. Comput. Phys. **114**, 185 (1994).
31. Z.-K. Qin, C.-S. Ma, D.-L, Li, D.-M. Zhang, and S.-Y. Liu, "Analysis for fabrication errors of arrayed waveguide grating multiplexers," Opt. Laser Tech. **40**, 235 (2008).

## 1. Introduction

Photonic crystals (PCs) have several applications such as line-defect PC waveguides (PCWs), coupled-resonator optical waveguides (CROWs) and reflectors, etc. due to the existence of photonic band gaps (PBGs) [1, 2, 3, 4]. Moreover, it is well known that self-collimated beams of light can propagate with almost no diffraction in PCs, and the bending and splitting of self-collimated beams have been realized [5, 6, 7, 8, 9]. PCs give reasonable promise of being the building blocks of photonic integrated circuits (PICs). In order to make practical use of such PICs, it is very important to find ways to couple them efficiently to conventional optical fibers and PCWs, and the discovery of enhanced transmission and highly directional emission of light (or beaming effect) from PCWs is one of the recent advances [10, 11, 12, 13, 14, 15, 16].

There are several methods to achieve the directional beaming from PCWs. Both enhanced transmission and strong beaming of light from a PCW can be obtained through appropriate corrugation or termination of the exit surface of PCW [10, 11, 12]. This beaming effect stems from the constructive interference of the emitted light beams from PCW and the leaky surface modes that can be supported at the surfaces of PC. Recently, the directional emission has been achieved by adding two point defects or by introducing CROWs near the exit surface of PCW [13, 14]. Furthermore, the beaming effect can be achieved by cascading a self-collimation PC to the PCW exit [15]. Recently, Li *et al.* demonstrated highly directional emission from PCWs by introducing the multiple output channels [16], which are constructed by taking ad-

#102911 - $15.00 USD Received 20 Oct 2008; revised 19 Nov 2008; accepted 21 Nov 2008; published 24 Nov 2008

vantage of the bending and splitting of light beams in PCWs [17, 18], near the exit surface of PCW. Besides, the directional emission from two adjacent parallel line-defect PCWs has been investigated [19], and very recently, Wang *et al.* reported that highly efficient directional emission using a coupled multi-channel structure to a PCW with surface modification can be achieved [20].

For all the above referred cases of directional emissions from PCWs, a precise alignment between the input light beams and narrow PCWs is still required to achieve high-efficiency coupling [10, 11, 12, 13, 14, 15, 16]. On the other hand, with a self-collimation-based directional emitter such a strict alignment condition is unnecessary for the coupling of the input light into the narrow PCWs [9, 19]. However, as it is unavoidable that the self-collimated beams of light in PCs spread transversely upon the emission out of PCs, achieving highly directional beaming from self-collimation PCs is also essential for efficient coupling to various optical components. Very recently, Liang *et al.* reported the directional emitter and compact beam splitters with a self-collimation PC by only modifying the surface structures [21].

In this paper, we present a new geometrical design in which three output channels are constructed by using the bending and splitting of self-collimated beams and by employing an antireflection coating (ARC)-like PC collimator. We will show that highly enhanced directional emission of self-collimated beams from PCs via three-point-source interference can be realized. In Section 2, the structures considered, together with the photonic band structures and their equifrequency contours (EFCs) are described. The results obtained for highly efficient beaming effects are presented in Section 3. The effects of alignment errors on the beaming characteristics are analyzed in Section 4.

## 2. Method and design

### *2.1. Photonic band structures and EFCs*

We consider two-dimensional (2D) square lattice PCs consisting of dielectric rods in air and restrict our consideration to the case of the TE modes (the electric field parallel to the rod axis). The dielectric constant and the radius of rods of PC 1 and 2 are $\varepsilon = 12.0$ and $r = 0.35\ a$, respectively, where $a$ is the lattice constant. The photonic band structure and the EFCs in the first band of the structures are calculated by the plane wave expansion method [22], and the results are shown in Figs. 1(a) and (b). The inset of Fig. 1(a) shows the structure of both PC 1 and 2. The frequencies of self-collimated light beams which propagate along the (11) direction (the ΓM direction) are around $f = 0.194\ c/a$, as shown by the EFCs of Fig. 1(b). It is shown that the $k_x$ values of flat dispersion region in which the self-collimation phenomenon occurs lie outside the EFC for air. In other words, because of the conservation of momentum component parallel to the interface, the self-collimated beams can be totally reflected at the PC–air interface in the (10) direction (the ΓX direction), opening the possibility of constructing the 90 ° bending structure [7, 8]. Moreover, a beam splitter (BS) which is based on the line-defect-induced bending effect [8], enables one to control the power ratio between the transmitted and reflected beams through the BS by varying the radius of rods in the line-defect and some values of which are listed in Table 1. Drawn in Figs. 1(c) and (d) are the photonic band structure and the EFCs in the second band of a PC collimator (PC 3), respectively, and the inset of Fig. 1(c) shows the structure of PC 3. The dielectric constant of PC 3 is the same as that of PC 1 and the radius of rods $r_c = 0.15\ a_c$, where $a_c$ is the lattice constant of PC 3. The frequencies of self-collimated light beams which propagate along the ΓX direction in PC 3 are around $f = 0.533\ c/a_c$, as shown by the EFCs of Fig. 1(d). The self-collimation frequencies of PC 1 are self-collimated in PC 3, yielding the enlargement of the lattice constant of PC 3 as $a_c = 2.747\ a$.

#102911 - $15.00 USD Received 20 Oct 2008; revised 19 Nov 2008; accepted 21 Nov 2008; published 24 Nov 2008

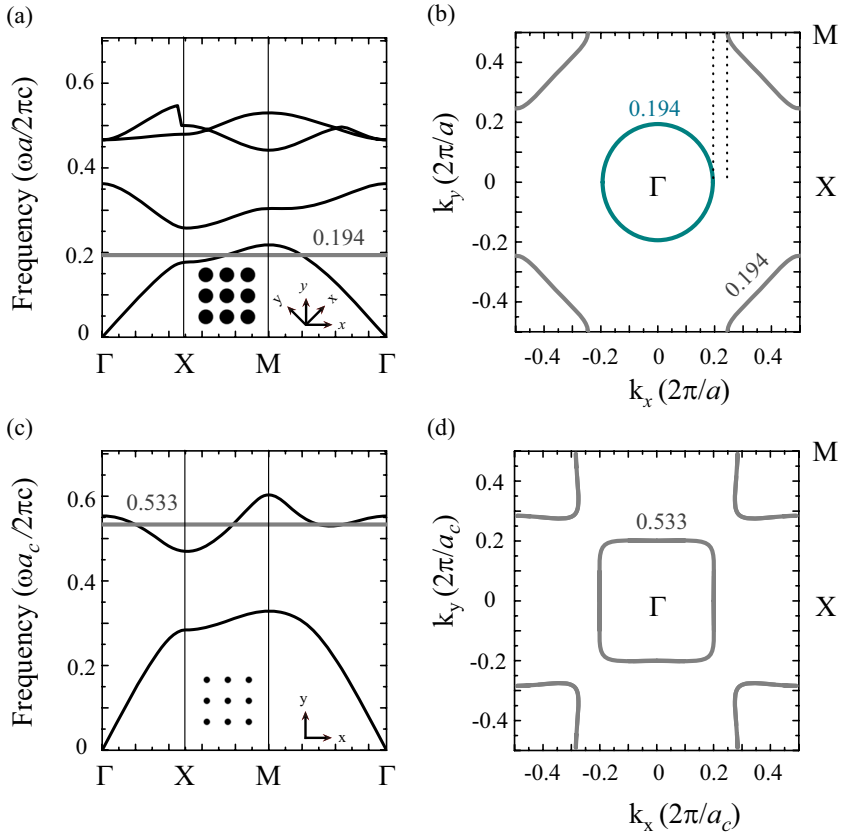


Fig. 1. Photonic band structures and EFCs of the 2D photonic crystals for the TE modes. The insets show the square PC structures, where the black circles represent the dielectric rods in air. The grey lines denote the self-collimation frequencies. (a) The first band structure and (b) the corresponding EFCs of the PC 1 and 2 at the self-collimation frequency $\omega = 0.194\ (2\pi c/a)$. The dielectric constant and the radius of rods are $\varepsilon = 12.0$ and $r = 0.35\ a$, respectively. The blue solid line denotes the EFC for air and the black dotted lines show the momentum components parallel to the PC–air interface in the ΓX direction. (c) The second band structure and (d) the corresponding EFCs of the PC 3 at the self-collimation frequency $\omega = 0.533\ (2\pi c/a_c)$. The dielectric constant and the radius of rods are $\varepsilon = 12.0$ and $r_c = 0.15\ a_c$, respectively.

#102911 - $15.00 USD Received 20 Oct 2008; revised 19 Nov 2008; accepted 21 Nov 2008; published 24 Nov 2008

Table 1. Ratio of transmitted to reflected power vs. the radius of defect rods $r_d$.

| $r_d$ $(a)$ | Power Ratio | Transmission (%) | Reflection (%) |
|---|---|---|---|
| 0.306 | 4 : 1 | 77 | 20 |
| 0.301 | 3 : 1 | 73 | 24 |
| 0.292 | 2 : 1 | 65 | 33 |
| 0.275 | 1 : 1 | 49 | 48 |
| 0.252 | 1 : 2 | 32 | 65 |
| 0.237 | 1 : 3 | 24 | 73 |
| 0.224 | 1 : 4 | 19 | 78 |

### *2.2. Design of efficient beaming structures*

Figure 2 shows various PC structures considered in this study. Figures 2(a)–(d) will be used as reference structures for investigating the beaming effect. In Fig. 2(a), the size of PC 1 with the radius of rods $r = 0.35\ a$ is set to the width $\mathrm{x} = 9\sqrt{2}\ a$ and the breadth $\mathrm{y} = 19\sqrt{2}\ a$. In Fig. 2(b), the ARC structures composed of the 7 small surface rods are introduced at each end of the central ports of 2D PC to improve the power transmission via the optimal minimization of the impedance mismatch between the PC and air [23]. The radius of the smaller rods $r_s = 0.2054\ a$ and the distance $d_s = 0.748\ a$ between the ARC structure and the truncated PC 1 are obtained by using the finite-difference time-domain (FDTD) simulations [24]. In Fig. 2(c), there are three layers at the exit surface with the central output layer positioned at one level lower. Here the small surface rods have the same values of $r_s$ and $d_s$ as in Fig. 2(b). In Fig. 2(d), a PC collimator (PC 3) with $N_\mathrm{x} = 3$ and $N_\mathrm{y} = 11$ layers is cascaded to the exit surface of PC 1 structure shown in Fig. 2(c), where $N_\mathrm{x}$ and $N_\mathrm{y}$ are the number of layers in the x- and y-directions, respectively. Efficient beaming emission via the self-collimation effect is obtained by achieving the maximum transmission of light beams through the Fabry-Pérot (FP) resonance condition [15]

$$\Delta\phi = \mathrm{k}d = m\pi\ (m = 1, 2, \ldots). \tag{1}$$

From Fig. 1(d), the wave vector in the ΓX direction is about $\mathrm{k} = 0.2\ (2\pi/a_c)$, then the minimum thickness $d$ of FP-like PC collimator is 2.5 $a_c$ to satisfy the above condition. The effective thickness of the PC collimator with $N_\mathrm{x}$ layers is $d_{eff} = (N_\mathrm{x} - 1)a_c + 2r_c$ and setting $N_\mathrm{x} = 3$ yields $d_{eff} = 2.3\ a_c$. $N_\mathrm{y} = 11$ is set for exciting two side lobes together with the main lobe of self-collimated light beam. The directional beaming via the interference between the main and the two lateral lobes of light beam is expected as in Ref. 15. The distance between the PC 1 and the PC collimator is set to $L = a/\sqrt{2}$. The minimum value of $L$ is required to minimize the spreading of light beam and achieve the best beaming effect.

Figures 2(e) and (f) represent the two newly designed structures to obtain highly directional emission, in which both a $V$-shaped BS and two 90° bending structures (or mirrors, Ms) are employed to introduce three output channels into the PC 2 structure. At the total internal reflection Ms (i.e., the PC 2–air interfaces in the ΓX direction), the Goos-Hänchen (GH) effect which refers to a lateral shift between the center of a reflected light beam and that of the incident beam is observed [25, 26], and the amount of shift measured is about 2 $a$. The BS consists of 15 defect rods with the radius $r_d = 0.301\ a$ and the ratio of transmission to reflection is 3 : 1. The beaming effect is investigated for the various ratios of transmission to reflection, as listed in Table 1, but the most efficient beaming is obtained at the ratio of 3 : 1 in the present designs; the intensities of the main lobe and each of the two lateral lobes of light beam are 75% and 12.5%,

#102911 - $15.00 USD Received 20 Oct 2008; revised 19 Nov 2008; accepted 21 Nov 2008; published 24 Nov 2008

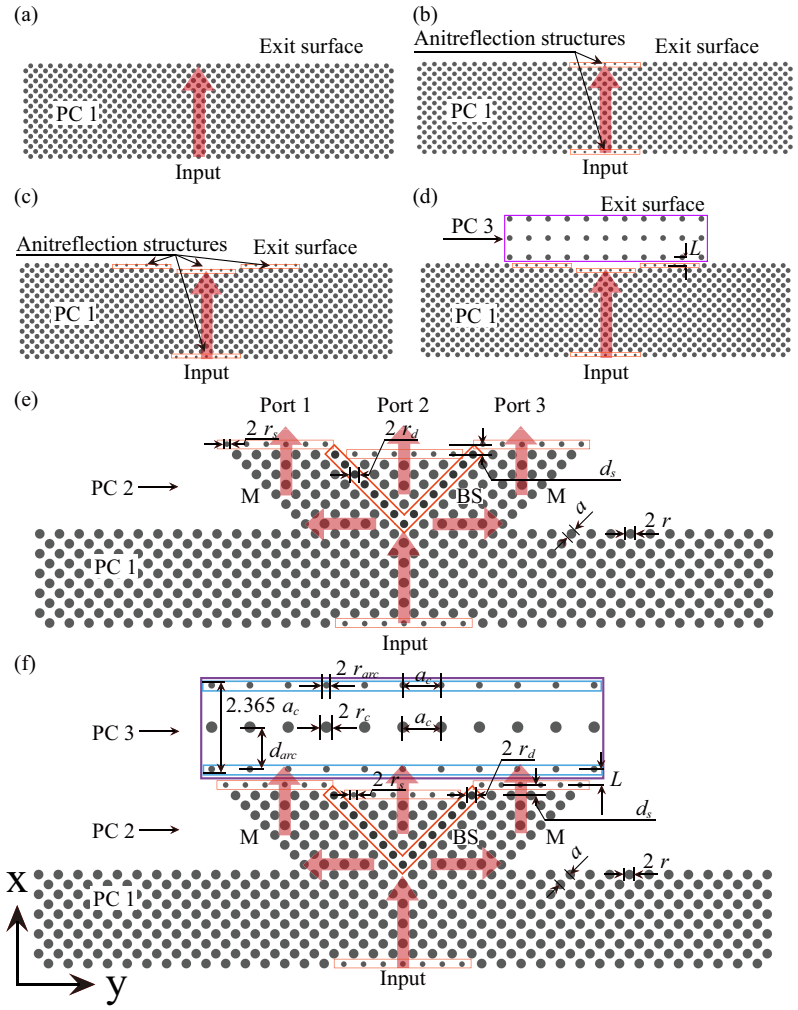


Fig. 2. Schematic diagrams of the photonic crystal structures under study. (a) PC 1 of the width x $= 9\sqrt{2}\,a$ and the breadth y $= 19\sqrt{2}\,a$, with the radius of rods $r = 0.35\,a$. (b) PC 1 with the ARC structures for both the central input and output ports, which are enclosed by the orange rectangle. The ARC parameters are the radius of rods $r_s = 0.2054\,a$ and the distance $d_s = 0.748\,a$ between the ARC structure and the PC truncation. (c) The exit surface is composed of three layers, where the ARC structures are employed. The central output port is one level lower than the PC surface layer. (d) PC 3 cascaded to the exit surface of PC 1 shown in (c). The size of PC 3 is set to $N_x = 3$ and $N_y = 11$, where $N_x$ and $N_y$ are the number of layers in the x- and y-directions, respectively. The lattice constant of PC 3 is $a_c = 2.747\,a$ and the radius of rods is $r_c = 0.15\,a_c$. The distance between PC 1 and 3 is chosen as $L = a/\sqrt{2}$. (e) The structure A: PC 2 cascaded to the exit surface of PC 1. PC 2 has three output channels constructed by using two mirrors in the ΓX direction and a $V$-shaped beam splitter with the radius of defect rods $r_d = 0.301\,a$. The ratio of transmission to reflection at the BS is 3 : 1. (f) The proposed structure B: the combined structure of PC 1, 2 and 3 with $N_x = 3$ and $N_y = 11$. The parameters for the ARC structures which are boxed with blue lines are the radius of rods $r_{arc} = 0.2485\,a$ and the distance $d_{arc} = 3.0\,a$. The distance between PC 2 and 3 is $L = a/\sqrt{2}$.

#102911 - $15.00 USD Received 20 Oct 2008; revised 19 Nov 2008; accepted 21 Nov 2008; published 24 Nov 2008

Table 2. Initial phase difference $\Delta\phi_{ij}$ vs. the number $N_{rm}$ of the removed central surface layers of PC 2.

| $N_{rm}$ | $\Delta\phi_{12} = -\Delta\phi_{23}$ | $\Delta\phi_{13}$ |
|---|---|---|
| 0 | 7.138 $\pi$ (or 1.138 $\pi$) | 0 |
| 1 | 7.584 $\pi$ (or 1.584 $\pi$) | 0 |
| 2 | 8.029 $\pi$ (or 2.029 $\pi$) | 0 |

respectively. The incident light beams through the path to Port 1 (or 3) experience a relative phase lag of $\pi/2$ at the BS and $\pi$ at the M [27, 28, 29], respectively. The distance among three output channels which is shown by red arrows in Figs. 2(e) and (f) is about $6\sqrt{2}\,a$.

The first design which is shown in Fig. 2(e) is the structure A where the PC 2 described above is cascaded to the exit surface of PC 1 structure. All the surface rods of PC 2 are smaller ones with the radius $r_s = 0.2054\,a$ and the distance $d_s = 0.748\,a$ and these function as an ARC layer. Here the central 7 surface rods of Port 2 are removed, and thus there are the 6 small surface rods on the next central surface layer of PC 2, thus Port 1 and 3 have one more layer than Port 2. Therefore, the difference between the optical path length (OPL) to Port 2 and that to Port 1 (or 3) for the incident light source from PC 1 is about $6.5\sqrt{2}\,a$, where the GH lateral shift of the reflected beam is also counted into [25]. In the structure A, the interference between the main and the two lateral lobes of light beam is analogous to three-point-source interference [When self-collimated beams radiate out of the end of PCs into air, they are diffracted with wide angular spread as can be seen in Figs. 3(a)–(c). And the widths of the main and two lateral lobes at the exit surface of PC 2 are 4.6 $a$ and 2.3 $a$, respectively, which are much smaller compared with the distance of observation which ranges from 30 $a$ to 100 $a$ away from the exit surface layer], whereupon the total irradiance is

$$I = I_1 + I_2 + I_3 + 2\sqrt{I_1 I_2}\cos\delta_{12} + 2\sqrt{I_2 I_3}\cos\delta_{23} + 2\sqrt{I_3 I_1}\cos\delta_{31}, \tag{2}$$

where

$$I_i = \frac{P_i}{2\pi r_i}, \;\; i = 1,2,3, \tag{3}$$

$$P_1 = P_3 = 0.125, \;\; P_2 = 0.75, \tag{4}$$

and

$$\delta_{ij} = \mathrm{k_{air}}\,(r_i - r_j) + \Delta\phi_{ij}, \;\; i,j = 1,2,3. \tag{5}$$

Here $I_i$ is the intensity at the point of observation arising from the light beam (or source) at Port $i$, $r_i$ the distance from Port $i$ to the point of observation, $P_i$ the power of light beam (or source) at the Port $i$. $\delta_{ij}$ is the total phase difference arising from the combined differences of initial phase and OPL in air to the point of observation for the sources at Port $i$ and $j$, $\mathrm{k_{air}}$ is the wave vector in air, and $\Delta\phi_{ij}$ is the initial phase difference between the sources at Port $i$ and $j$. From Fig. 1(a), the wave vector of light beams with the self-collimation frequency $f = 0.194\,c/a$ is about $\mathrm{k}_{sc} = 0.509\,(2\pi/a)$ in the ΓM direction of PC 1 (or PC 2), which corresponds to the wavelength of about $\lambda_{sc} = 1.965\,a$, and $\mathrm{k_{air}} = 0.194\,(2\pi/a)$ in air. The initial phase difference $\Delta\phi_{ij}$ can be controlled by varying the central surface layer level of Port 2, as listed in Table 2. The values given in Eq. (6), i.e., the case in which one central surface layer of Port 2 is removed ($N_{rm} = 1$), yield the best results for the desired beaming effect.

$$\Delta\phi_{12} = -\Delta\phi_{23} = 7.584\,\pi\ (\text{or } 1.584\,\pi), \text{ and } \Delta\phi_{13} = 0. \tag{6}$$

#102911 - $15.00 USD Received 20 Oct 2008; revised 19 Nov 2008; accepted 21 Nov 2008; published 24 Nov 2008

The second structure B which is shown in Fig. 2(f) is a novel design proposed to obtain highly efficient beaming and has been designed in two steps. Firstly, the same design as the structure A is employed. Secondly, a PC collimator (PC 3) is added near the exit ports of PC 2. For the distance between PC 2 and 3, the value of $L = a/\sqrt{2}$ is chosen for the same reasons as for the structure shown in Fig. 2(d). The size of PC 3 is set to $N_{\mathrm{x}} = 3$ and $N_{\mathrm{y}} = 11$. The PC collimator (PC 3) in this structure is different from the FP-like PC collimator shown in Fig. 2(d) [Only the one middle layer in the x-direction is a part of PC 3 shown in Fig. 2(d) (i.e., with the same lattice constant $a_c$ and the radius $r_c$) and the two side layers composed of smaller rods are the ARC structures. We name the PC collimator introduced here the 'ARC-like PC collimator']. When the value of $N_{\mathrm{x}}$ is varied from 3 to 8, all the ARC-like PC collimators are observed to yield nearly perfect transmissions. Thus, the value $N_{\mathrm{x}} = 3$ is chosen for achieving the minimum size PC collimator which exhibits almost perfect transmission [99.7% transmission of incident light beam, which is achieved with the ARC structures added]. The ARC parameters, the radius of rods $r_{arc}$ and the distance $d_{arc}$ between the ARC structure and the truncated PC 3 (i.e., the semi-infinite PC 3) are optimized by using the FDTD simulations. It is found that at $r_{arc} = 0.2485\,a$ and $d_{arc} = 3.0\,a$ the reflectance becomes almost zero (about 0.0002) [with $|r_{12}| = |r_{23}| = 0.674$, where the symbols $r_{12}$ and $r_{23}$ are quoted from Ref. 23. Here $|r_{12}|$ is the amplitude of the reflection coefficient of the ARC structure and $|r_{23}|$ is that of the semi-infinite PC 3]. The value of $N_{\mathrm{y}}$ is the same as that of the PC collimator shown in Fig. 2(d). In this case, two side lobes in addition to the central emission lobe are actively generated by three output channels constructed in the structure A; highly efficient beaming effect via the interference between the main and the two lateral lobes of light beam is enhanced by the utilization of the combined advantages of the structure A and the ARC-like PC collimator.

## 3. Simulation results and analysis

Using the FDTD method with the perfectly matched layers which are absorption boundaries [30], the emission properties of the structures are investigated quantitatively. Figure 3 displays the electric-field amplitude distributions obtained for the corresponding PC structures depicted in Fig. 2. The spatial resolution $\triangle x$ in the computational domain is set to $a/32$ and then the time step $\triangle t$ is given by $\triangle t = S\triangle x/c < (1/\sqrt{2})\triangle x/c$, where the Courant factor $S$ is chosen as $S = 0.704$, in order for the FDTD method to be stable (not diverge). The software used, RSOFT FullWAVE, has an averaging function (i.e., the average of refractive index near the boundaries). The FDTD simulation gives a clear distinction for the design features smaller than the spatial resolution $\triangle x$. In the simulations, the Gaussian TE mode light source with the width of $4\,a$ is launched at the distance of $\sqrt{2}\,a$ before the center of the input surface layer of PC 1 and propagates along the x-direction at the plane $\mathrm{y} = 0$, where $\mathrm{x} = 0$ is positioned at the exit surface layer of PC 1 in Figs. 3(a), (b) and (c), of PC 2 in Fig. 3(e) and of PC 3 in Figs. 3(d) and (f). The operating frequency $f = 0.194\,c/a$ which represents the frequency of self-collimated light beams propagating along the ΓM direction in PC 1 corresponds to $f = 0.533\,c/a_c$, the frequency of self-collimation along the ΓX direction in PC 3.

The FDTD simulation results are obtained as follows: the transverse time-averaged transmission coefficients of power in the range of $|\mathrm{y}| \leq 40\,a$ are measured from $\mathrm{x} = 10\,a$ to $\mathrm{x} = 100\,a$ with an interval of $10\,a$, and to characterize the directional beaming effect in more detail, the time-averaged transmission coefficients of power (normalized by the incident power) along the x-direction are calculated within $|\mathrm{y}| \leq 8.24\,a$ (or $3\,a_c$) at the positions of $\mathrm{x} = 10ma$ $(m = 0, 1, 2, \ldots, 10)$.

Figures 3(a) and (b) show the FDTD simulated field distributions of direct emission (only with PC 1) at steady states. The direct emission of self-collimated beams from PCs is diffracted with wide angular spread just as expected. More enhanced transmission is observed in Fig. 3(b)

#102911 - $15.00 USD Received 20 Oct 2008; revised 19 Nov 2008; accepted 21 Nov 2008; published 24 Nov 2008

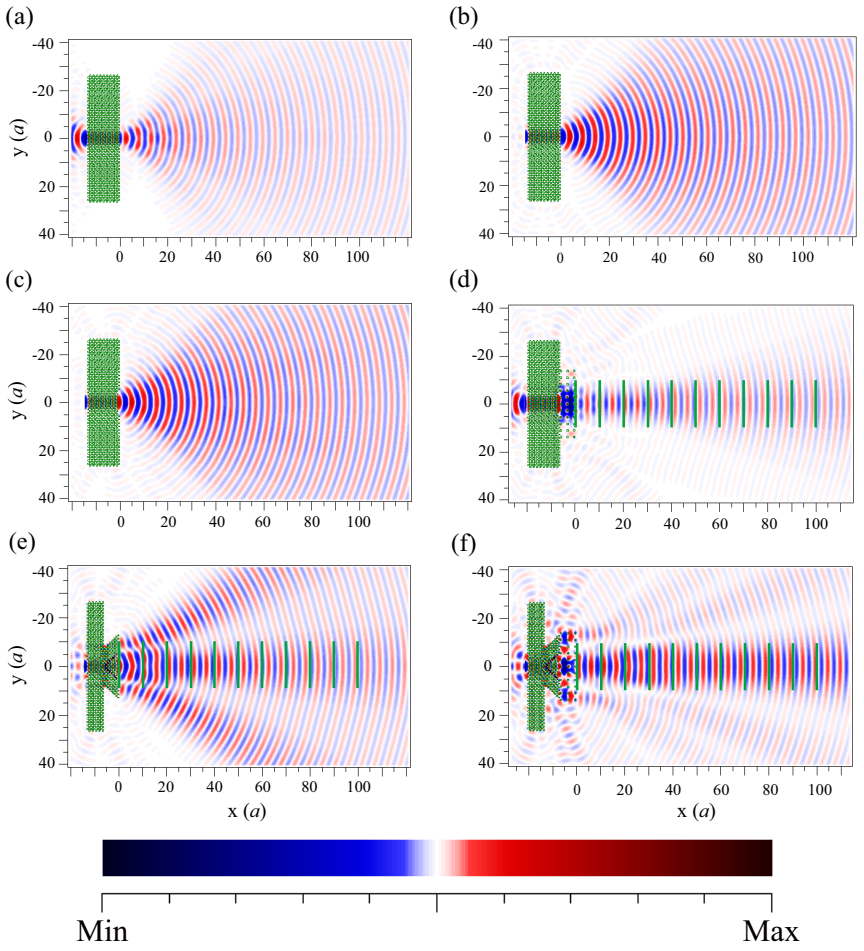


Fig. 3. Optical field amplitude distributions for the corresponding PC structures shown in Fig. 2. The frequency and width of the incident beam are $f = 0.194\ c/a$ and 4 $a$, respectively. The green long lines drawn in Figs. (d)–(f) denote the detector positions to measure the power transmitted along the x-direction.

#102911 - $15.00 USD Received 20 Oct 2008; revised 19 Nov 2008; accepted 21 Nov 2008; published 24 Nov 2008

than in Fig. 3(a), confirming the fact that small surface rods introduced function as an antireflection layer between the PC structure and air to minimize the reflection of light beam [23]. It is also noticeable that Fig. 3(c) shows the reduced range of diffraction angles compared with Fig. 3(b) although Fig. 3(c) shows less enhanced transmission compared with Fig. 3(b). In Fig. 3(d), one can see that the directional beaming is clearly achieved up to about x $= 80\,a$ (or 15.6 $\lambda_{\text{air}}$), but the power transmission is very low compared with the results shown in Figs. 3(b) and (c). In other words, the FP-like PC collimator in this structure is not properly optimized so that no more than 31% of incident light beam is transmitted through this collimator. Comparison of Figs. 3(b)–(d) suggests that there may be a trade-off between the transmission and the directionality of power, as mentioned in Ref. 13. The simulated field distributions for the structures A and B are depicted in Figs. 3(e) and (f), respectively. The directional emission in both cases is more enhanced than in the case of Fig. 3(d), which is attributable to the interference of light beams from the three output channels [13]. Important parameters considered in the present designs of the two structures are the ratio of transmission to reflection in the *V*-shaped BS, the distances between the ports, the initial difference between the OPLs to each port, the antireflection structure, and/or the ARC-like perfectly transmitting PC collimator. In the present designs, the results shown in Figs. 3(e) and (f) are the best we could achieve although there is still some spread of power from the central beam.

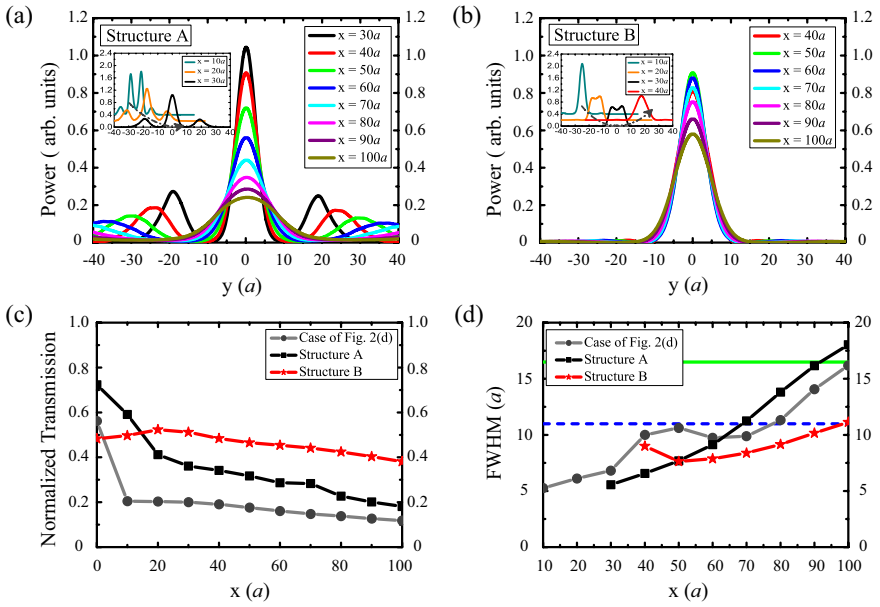


Fig. 4. Transverse time-averaged power transmission for (a) the structure A and (b) the structure B. The insets show the transmitted power patterns at short distances. (c) Time-averaged power transmissions within $|y| \leq 8.24\,a$ (or $3\,a_c$) along the x-direction for the structures A, B and the one shown in Fig. 2(d). (d) FWHM data of the transmitted power patterns for the three structures in (c). The green solid line indicates the width of about 16.48 $a$ (or 6 $a_c$) and the blue dashed line the width of about 10.99 $a$ (or 4 $a_c$) which is the width of self-collimated beams in PC 3. Here x $= 0$'s are the positions of the immediate exit surface of PC 2 and 3 (see Figs. 3(d)–(f)).

Figures 4(a) and (b) show the transverse time-averaged transmission coefficients of power, and in the insets the transmitted power patterns at short distances are displayed. In Fig. 4(a), the

#102911 - $15.00 USD Received 20 Oct 2008; revised 19 Nov 2008; accepted 21 Nov 2008; published 24 Nov 2008

total irradiances of light beam in the x-direction at the positions of Port 1 and 3 (or $y = \pm 6\sqrt{2}\,a$) are almost minima and at Port 2 (or $y = 0$) maxima, and thus at the position of about $x = 30\,a$, two nodes where the waves have minimal amplitudes are clearly seen at about the positions of Port 1 and 3. The maximum transmitted powers of lateral lobes are about a fifth the power of the main emission lobe and the positions of lateral lobes move farther away from the main lobe as the emitted light beam propagates, which are consistent with the results obtained from the above Eqs. (2)–(6). In Fig. 4(b), an enhanced beaming of emitted light is realized almost without the transmitted power of lateral lobes. In the figure, one can observe that although the powers at $x = 40\,a$ and $50\,a$ are comparable to the values obtained for the structure A, the transmitted powers at farther distances are much stronger. The power distribution displayed in Fig. 4(b) is the best result obtainable with the present design. For the three PC structures shown in Figs. 2(d)–(f), the time-averaged transmission coefficients of power along the x-direction calculated within $|y| \leq 8.24\,a$ (or $3\,a_c$) are drawn in Fig. 4(c) for comparison. The transmitted power decreases from 36% (51%) at $x = 30\,a$ to 20% (40%) at $x = 90\,a$ for the structure A (B). The structure B exhibits markedly better results than the structure A with respect to the transmission of power. Figure 4(d) shows the full-width at half-maximums (FWHMs) of the directional emitting beam for the structures in Figs. 2(d)–(f). In the structure A, the FWHM less than $16.48\,a$ (or $6\,a_c$) is maintained up to about $x = 90\,a$ (or $17.5\,\lambda_{\text{air}}$), while for the structure B the FWHM of $10.99\,a$ (or $4\,a_c$, the width of self-collimated beams in PC 3) is maintained up to about $x = 100\,a$ (or $19.4\,\lambda_{\text{air}}$). These results are better than that of Ref. 15 where the directional beaming is achieved through the distance of $12.6\,\lambda_0$ with $\lambda_0$ the wavelength in vacuum. The structure B shows much improved performance of directional beaming, i.e., the width of emitting light beam in the structure B is far narrower than in the structure A. From the comparison of the two figures, Figs. 4(c) and (d), the structure B may be considered as one of the major breakthroughs against the trade-off between the transmission and the directionality of power at distances farther than about $x = 30\,a$ (or $5.8\,\lambda_{\text{air}}$).

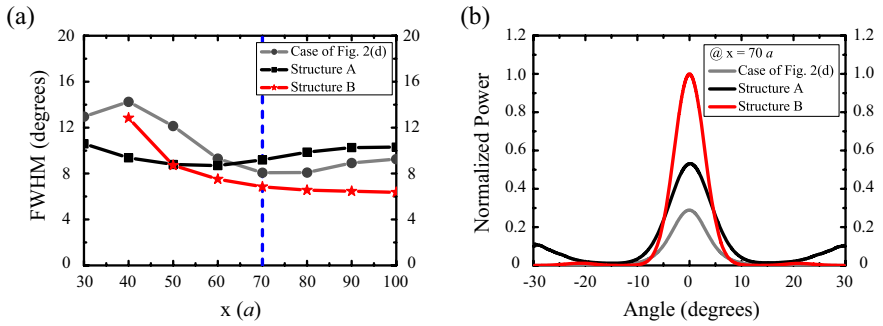


Fig. 5. (a) Angular FWHMs of power patterns for the structures A, B and that of Fig. 2(d). The blue dashed line indicates the position of $x = 70\,a$. (b) Comparison of angular power transmissions for the structures A, B and that of Fig. 2(d) at $x = 70\,a$.

Figure 5(a) exhibits the angular FWHM data of radiation patterns for the three structures shown in Figs. 2(d)–(f). The blue dashed line indicates the position of $x = 70\,a$ (or $13.6\,\lambda_{\text{air}}$) at which the FWHMs are 9.2° and 6.9° for the structures A and B, respectively [8.1° for the structure of Fig. 2(d)]. For highly directional emission of light from PCWs, the angular FWHMs of 5° and below have been achieved in Refs. 10, 12 and 16. The reason that our FWHM results are worse might be more or less due to the fact that the wavelength of input source in this study is about twice larger [12]. On the other hand, our results are superior to that of Ref. 13

#102911 - $15.00 USD Received 20 Oct 2008; revised 19 Nov 2008; accepted 21 Nov 2008; published 24 Nov 2008

where the beaming effect from PCW is achieved by adding two or four point defects and the smallest angular spread of emitting beam is around 16°. In addition, our results are much better compared with that of Ref. 21 in which a similar directional emission of self-collimated beam from PC is reported and the smallest divergence angle is about 21.4°. Comparison of angular power transmissions for the structures A, B and that of Fig. 2(d) at the position of x = 70 $a$ is also plotted in Fig. 5(b). The beaming characteristics are clearly seen in Figs. 5(a) and (b), and the underlying mechanism lies in the interference of self-collimated light beams from three output channels of PC 2 and/or the ARC-like perfect transmission of PC collimator.

## 4. Device sensitivity to the alignment errors

The proposed beaming structure is novel and can be used for highly efficient coupling of self-collimated beams from PCs into conventional optical fibers and PCWs. From the point of view of the fabrication to realize this device, the efficiency of beaming should be insensitive to the alignment and the allowed fabrication errors [31] should be investigated. In this study, we only investigated the device sensitivity to the transverse alignment error [19] and the tilt error of the ARC-like PC collimator. Due to the symmetry of the PC structure, we just discuss the tilt angle $\theta$ of the ARC-like PC collimator varied counter-clockwise about the rod axes of the collimator at the plane y = 0 for the tilt error, and the ARC-like PC collimator varied positively for the transverse alignment error. Here the tilt angle is limited up to 1.0° due to the distance between PC 2 and the ARC-like PC collimator $a/\sqrt{2}$.

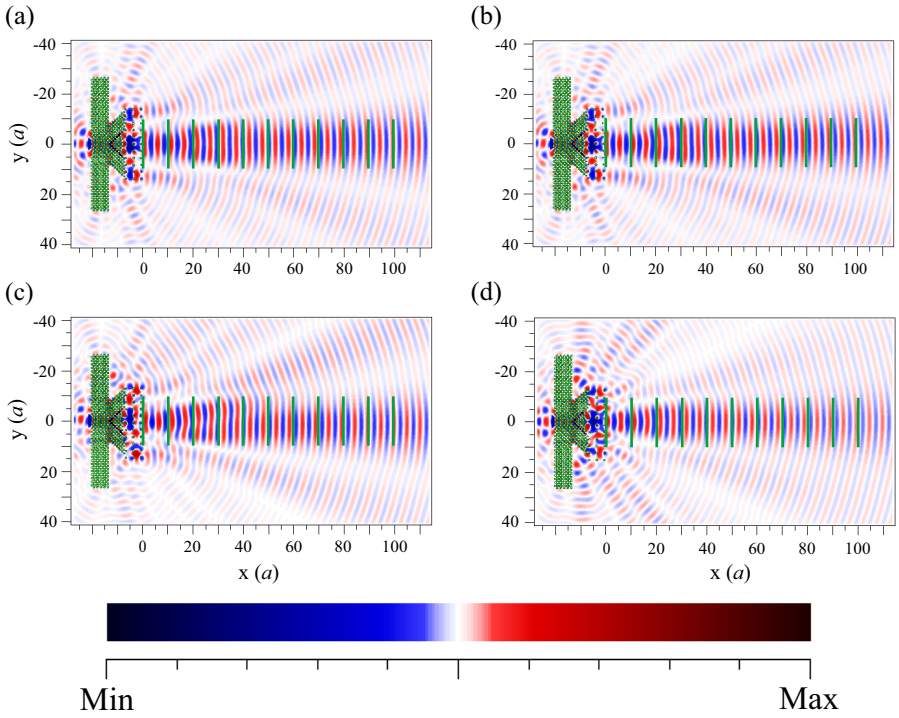


Fig. 6. Optical field amplitude distributions for (a) the tilt error of 0.5°, (b) of 1.0°, (c) the transverse alignment error of $a/\sqrt{2} = 0.7071\ a$, and (d) of $a_c/2 = 1.3735\ a$. The green long lines drawn denote the detector positions to measure the power transmitted within $|y| \leq 8.24\ a$ (or 3 $a_c$) along the x-direction, as in Fig. 3.

#102911 - $15.00 USD Received 20 Oct 2008; revised 19 Nov 2008; accepted 21 Nov 2008; published 24 Nov 2008

Figure 6 shows the FDTD simulated field distributions for the four alignment errors. It can be found that the tilt errors of $0.5^\circ$ and $1.0^\circ$ have little effect on the beaming, as shown in Figs. 6(a) and (b), respectively. For the transverse alignment error of $a/\sqrt{2} = 0.7071\ a$ in Fig. 6(c), a slight rightward deflection can be found, which is due to the asymmetrical characteristic of coupling scheme. While, for the transverse alignment error of $a_c/2 = 1.3735\ a$ in Fig. 6(d), there is almost no deflection due to the symmetrical characteristic of coupling scheme, but the transmission of power diminishes due to the asymmetrical characteristic of the ARC-like PC collimator with respect to PC 2.

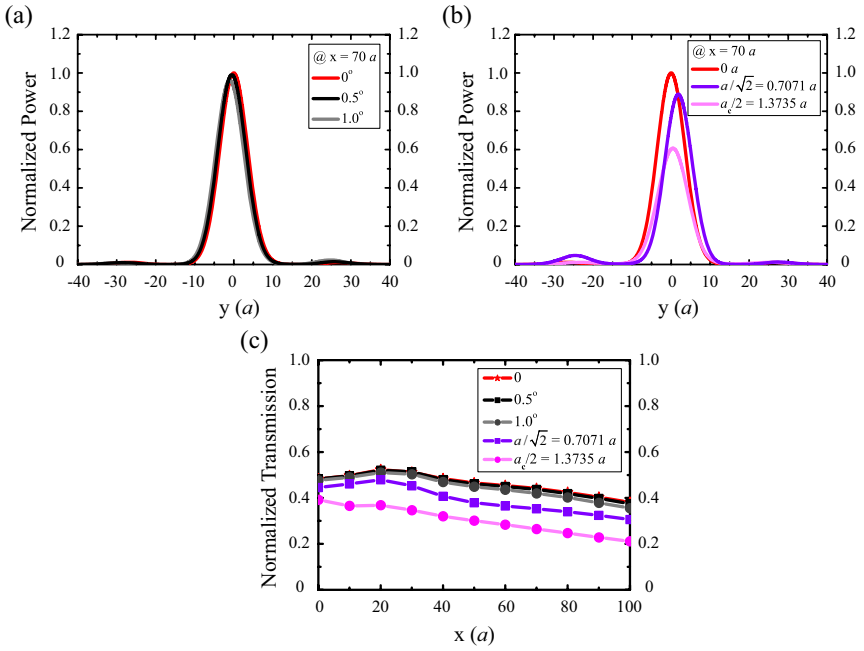


Fig. 7. Transverse time-averaged power transmissions at the position of x = 70 $a$ for (a) the tilt errors and (b) the transverse alignment errors. (c) Time-averaged power transmissions within $|y| \leq 8.24\ a$ (or 3 $a_c$) along the x-direction for the four cases of alignment errors.

Figures 7(a) and (b) show the transverse time-averaged transmissions of power (normalized by the peak power in the case of no alignment error) for the tilt and alignment errors at the position of x = 70 $a$ (or 13.4 $\lambda_{\text{air}}$), respectively. It can be found that the tilt errors hardly affect the efficiency of the directional beaming, although there is an insignificant leftward deflection and the corresponding small side lobes appear in Fig. 7(a). The FWHMs are 8.38 $a$, 8.44 $a$ and 8.47 $a$ for the cases of no alignment error, the tilt errors of $0.5^\circ$, and of $1.0^\circ$, respectively. For the transverse alignment errors shown in Fig. 7(b), there is a slight rightward deflection in the case of the transverse alignment error of $a/\sqrt{2} = 0.7071\ a$, which results in the shift of the center of beaming. The amount shifted is 1.84 $a$ rightward. And the corresponding small side lobes appear at the position of $y = -24.63\ a$. In the case of the transverse alignment error of $a_c/2 = 1.3735\ a$, the transmitted power decreased is about a half the power in the case of no alignment error. The FWHMs are 8.38 $a$, 8.28 $a$ and 9.06 $a$ for the cases of no alignment error, the transverse alignment errors of $a/\sqrt{2} = 0.7071\ a$, and of $a_c/2 = 1.3735\ a$, respectively. For the four alignment errors, the time-averaged power transmission coefficients within $|y| \leq 8.24\ a$ (or 3 $a_c$) along the x-direction are drawn in Fig. 7(c) for comparison. At the

#102911 - $15.00 USD Received 20 Oct 2008; revised 19 Nov 2008; accepted 21 Nov 2008; published 24 Nov 2008

position of x = 70 a, the transmitted powers are 44.1%, 43.7%, 42.0%, 35.3% and 26.5% for the cases of no alignment error, the tilt errors of $0.5^\circ$, of $1.0^\circ$, the transverse alignment errors of $a/\sqrt{2} = 0.7071\,a$, and of $a_c/2 = 1.3735\,a$, respectively. It can be found that the efficiency of the directional beaming is almost insensitive to the tilt errors of $0.5^\circ$ and $1.0^\circ$, and the transmitted power for the case of the transverse alignment error of $a/\sqrt{2} = 0.7071\,a$ is larger than 80% of the value obtained for the case of no alignment error. We conclude that the directional emission efficiency is almost insensitive to the tilt errors of $|\theta| \leq 1.0^\circ$, and the transverse alignment errors within $|\mathrm{x}| \leq 0.7071\,a$ are acceptable [19].

The effects of the fabrication errors on the transmission and beaming of light are not considered in the present work. The fabrication errors may have great impact on the device performances and the detailed analysis for the fabrication errors may be the issue of future work.

## 5. Conclusion

We have designed two new structures to achieve highly directional beaming of self-collimated beams from PC structures. The main mechanism lies in the interference of light beams from three output channels constructed by using the bending and splitting of self-collimated beams and in the effective suppression of reflected light beams by employing the concept of ARC structures at the interfaces. One structure (the structure B) contains a ARC-like PC collimator (PC 3) which is added to the exit surface of PC 2, and the other (the structure A) doesn't. Using the FDTD method, we obtained the emission properties such as the field patterns and the transmission coefficients of power as well as the angular distributions of power transmitted. It is demonstrated that the structure B is a novel design which we propose for achieving both enhanced transmission and highly directional emission of self-collimated beams from photonic crystals. The beaming efficiency is almost insensitive to the tilt errors of $|\theta| \leq 1.0^\circ$ and the transverse alignment errors within $|\mathrm{x}| \leq 0.7071\,a$ are acceptable. In view of the results obtained, this design can be used for the efficient coupling of self-collimated beams from PCs into conventional optical fibers and PCWs, and in other applications to achieve highly directional beaming.


## Acknowledgments

We would like to acknowledge the support of the Basic Research Program of KAIST.


#102911 - $15.00 USD Received 20 Oct 2008; revised 19 Nov 2008; accepted 21 Nov 2008; published 24 Nov 2008